RMetS

Royal Meteorological Society

Ultrahigh resolution wind forecasting for the sailing events at the Rio de Janeiro 2016 Summer Olympic Games

Theodore M. Giannaros,[a]* Vassiliki Kotroni,[a] Konstantinos Lagouvardos,[a] Dimitrios Dellis,[b] Panayiotis Tsanakas,[c] Gabriel Mavrellis,[d] Panagiotis Symeonidis[d] and Theodoros Vakkas[d]

[a] *National Observatory of Athens, Institute for Environmental Research and Sustainable Development, Athens, Greece*
[b] *Greek Research and Technology Network, Athens, Greece*
[c] *School of Electrical and Computing Engineering, National Technical University of Athens, Greece*
[d] *Geospatial Enabling Technologies (GET), Athens, Greece*

ABSTRACT: The current study presents AEOLUS-RIO2016, an ultrahigh resolution wind forecasting system that was developed and implemented operationally for supporting the Hellenic Olympic Sailing Team during the sailing events at the Rio de Janeiro 2016 Summer Olympic Games. The forecasting system was built around the state-of-the-art numerical weather prediction Weather Research and Forecasting model, ported to a high performance computing infrastructure that ensured the reliability and timeliness of the provided service. Advanced web mapping tools were employed for communicating forecasts effectively to the athletes and coaches throughout the period of the sailing events. Prior to the operational deployment of AEOLUS-RIO2016, sensitivity experiments were carried out, focusing on the representation of topography and land use and aiming at improving wind forecasts. The results suggest that the employment of very high resolution and up-to-date terrestrial data allowed model performance to be improved, especially in terms of the wind direction guidance provided. Considering the period of the sailing events, the evaluation of AEOLUS-RIO2016 revealed an overall satisfactory performance. Notably, however, it was found that the system failed to provide reliable wind guidance on specific days. *A posteriori* implementation of the model using an alternative source for providing initial and lateral boundary conditions showed notable improvements in model performance.

KEY WORDS   Rio 2016 Olympic Games; wind; sailing; ultrahigh resolution; WRF; high performance computing

Received 28 November 2016; Revised 21 March 2017; Accepted 29 March 2017

1. Introduction

Back in the late 1970s, Thorne (1977) documented the diverse effects weather has on sport. Since then, extensive research has been conducted focusing on how weather and environmental conditions influence various sports and athletes' performance (e.g. Cairns, 1984; Schroter and Marlin, 1995; Spellman, 1996; Diafas *et al.*, 2006; Ely *et al.*, 2007; Morris and Phillips, 2009; Pezzoli *et al.*, 2010, 2012; Matzarakis and Fröhlich, 2015). Among the sports that are most heavily affected by weather conditions, sailing is a characteristic example. For instance, it is well known that sailing routes in competitive events are defined based on wind direction, while wind speed determines when a race will start or be cancelled. Gaining knowledge about wind conditions is of paramount importance to sailors, who need to set up an effective strategy before a race and elaborate quick strategic and tactical decisions once the race begins (Houghton and Campbell, 2008; Bethwaite, 2011). Therefore, it is understandable why, at top sports level, sailing teams rely on meteorologists for obtaining reliable wind information (Pezzoli and Bellasio, 2014). For instance, the Australian Bureau of Meteorology set up an advanced wind forecasting service to support the sailing events at the 2000 Sydney Olympic and Paralympic Games

(Spark and Connor, 2004), while the Qingdao Meteorological Bureau employed numerical weather prediction models and statistical tools for supporting the sailing events at the 2008 Beijing Olympic and Paralympic Games (Ma *et al.*, 2013).

Sailing has been an Olympic sport since the beginning of the modern games that took place in Athens, Greece, in 1896. However, bad weather conditions postponed its debut until the 1900 Paris games. In the 2016 Summer Olympic Games, hosted by the city of Rio de Janeiro in Brazil, the sailing competitions took place at the Guanabara Bay between 8 and 18 August. During this period, 380 athletes from 66 countries competed in 10 different sailing events (http://www.rio2016.com/en/sailing). The National Observatory of Athens (NOA), in collaboration with Geospatial Enabling Technologies (GET) Ltd and the Greek Research and Technology Network (GRNET) SA, supported the Hellenic Olympic Sailing Team (hereafter referred to as HOST), composed of seven athletes competing in five events, with ultrahigh resolution weather forecasts with special emphasis on wind.

The primary aim of the NOA was to provide the members of the HOST with high-quality wind forecasts, tailored to their very specific needs. The key requirements included the timely delivery of the forecasts early in the morning, high temporal and spatial resolution, the development of a specific communication protocol and the setup of a user-friendly demonstration interface. To meet these requirements, a state-of-the-art numerical weather prediction (NWP) model was ported to a high performance computing (HPC) infrastructure. Advanced web mapping techniques

* Correspondence: T. M. Giannaros, National Observatory of Athens, Institute for Environmental Research and Sustainable Development, Vas. Pavlou & I. Metaxa, 15236 Athens, Greece. E-mail: thgian@noa.gr

were consequently exploited for setting up communication with the athletes and coaches of the HOST.

The current study therefore presents the development and evaluation of an ultrahigh resolution wind forecasting system designed to fulfil the needs of the Greek athletes who participated in the sailing events of the 2016 Olympic Games. The key objective was to highlight the added value that sport, and particularly sailing, can gain from the proper exploitation of NWP. The challenges faced and the associated lessons learned are anticipated to serve as a reference point for the development and/or improvement of similar meteorological applications in the future.

2. The NWP challenge

Guanabara Bay is one of the most prominent bays in southeast Brazil (Figure 1(a)). It is located in the Rio de Janeiro state, confined to the area between 22°40′S and 23°00′S latitude and 43°00′W and 43°18′W longitude (Figure 1(b)). The bay is one of the largest in Brazil with an estimated area of about 384 km² , including the islands (De Carvalho and Neto, 2016). The shape of the bay resembles a semi-circle and measures 30 and 28 km along the north−south and the west−east axis, respectively (Soares-Gomes *et al.*, 2016). According to the Koppen climate classification scheme, the climate of the region is Atlantic tropical (Aw), characterized by dry (June−August) and wet (December−April) periods with significant differences in the mean rainfall (INMET, 2015). Over the bay, winds blow predominantly from south and north directions, showing an average velocity of about 5 m s⁻¹. Southerlies tend to occur more frequently throughout the year and are most often associated with the passage of cold fronts (Soares-Gomes *et al.*, 2016). Thermal wind regimes (sea/land breezes) also influence the bay. In particular, winds from the eastsoutheast sector are associated with a sea breeze, while winds blowing from the northwest are influenced by the land breeze. Both sectors are important during spring and winter, although Zeri *et al.* (2011) have found that sea/land breezes exhibit higher velocities during the springtime than during the wintertime.

The sailing field of the Rio 2016 Olympic Games consisted of seven courses, as shown in Figure 1(c). Three of the racing areas were located at the exit of the Guanabara Bay, the courses of Copacabana (circle 1), Niteroi (circle 2) and Pai (circle 3), while the remaining four, Pao de Acucar (circle 4), Escola Naval (circle 5), Aeroporto (circle 6) and Ponte (circle 7), were located within the bay. Marina da Gloria, denoted with the star in Figure 1(c), was the official sailing venue during the games.

The intricate topography that surrounds the sailing areas (Figure 1(c)) poses a challenging NWP problem. The interaction of the synoptic flow with the local breezes driven by temperature and pressure gradients between the land and the ocean, superimposed over the highly complex topography and land−water distribution, result in notorious differences in wind direction and speed within the region (INMET, 2015). Such variations in wind may occur within distances of a few hundred meters and within periods of less than 30−60 min. This leads to the necessity of focusing on the meso-γ, and possibly on the micro-α, rather than on the meso-β scale (Fujita, 1986), which has traditionally been used in related operational weather forecasting activities (e.g. Rothfusz *et al.*, 1998; Spark and Connor, 2004). Ultrahigh resolution NWP could be a solution as long as attention is paid to the proper representation of the study area in terms of topography and land−sea contrast.

3. Details of the AEOLUS-RIO2016 forecasting service

Named after the ruler of the winds in Greek mythology, AEOLUS-RIO2016 is the forecasting service developed by the NOA in collaboration with GET Ltd and GRNET SA with the aim of supporting the HOST operationally during the 2016 Rio Olympic Games. The service comprises an ultrahigh resolution NWP system, ported to a HPC infrastructure and an advanced web mapping portal, employed for communicating products to the HOST's members.

3.1. The NWP system

AEOLUS-RIO2016 was built around the state-of-the-art NWP Weather Research and Forecasting (WRF) model, version 3.7.1 (Skamarock *et al.*, 2008). Four one-way nested modelling domains were used, with horizontal grid spacing of 25 km (mesh size of 160 × 100), 5 km (mesh size of 151 × 151), 1 km (mesh size of 121 × 121) and 200 m (mesh size of 121 × 116), of which the innermost ultrahigh resolution domain focused on the target area (Figure 1(c)). Forty unevenly spaced full sigma levels were defined in the vertical and the model top was set to 100 hPa. The one-way nesting approach was preferred over the two-way approach to avoid the occurrence of numerical instability due to the adopted ultrahigh horizontal grid spacing.

The Rapid Radiative Transfer Model (Mlawer *et al.*, 1997) and the Dudhia scheme (Dudhia, 1989) were selected for the parameterization of long wave and short wave radiation, respectively, while the Thompson parameterization (Thompson *et al.*, 2008) was chosen for the representation of microphysics. Processes in the planetary boundary layer were handled with the Mellor−Yamada−Janjic scheme (Janjic, 1994), and the Unified Noah Land Surface Model (Tewari *et al.*, 2004) was employed for the land surface. The Kain−Fritsch convective parameterization scheme (Kain, 2004) was selected for representing convection in the 25 and 5 km domains, whereas convection was explicitly resolved in the 1 km and 200 m domains. It should be noted that the combination of the Mellor−Yamada−Janjic planetary boundary layer scheme and the Noah Land Surface Model was decided on the basis of past experience with the WRF model, in particular focusing on the simulation of wind at high horizontal grid spacing (e.g. Kioutsioukis *et al.*, 2016; Koletsis *et al.*, 2016; Giannaros *et al.*, 2017).

The 0000 UTC 0.5° × 0.5° grid resolution and 6 h temporal resolution data of the Global Forecast System (GFS) and high resolution (0.083° × 0.083°) sea-surface temperature analyses, provided by the National Centers for Environmental Prediction (NCEP), were used for initializing the WRF model. Numerical forecasts were conducted operationally for the period between 1 June and 18 August 2016. Forecasts were initialized at 0000 UTC of each day and extended to 48 h, providing output at 30 min intervals. To address the high computational demands of the NWP system and the necessity to deliver timely forecasts, the NWP system was ported to ARIS (Advanced Research Information System), a HPC infrastructure operated by GRNET.

ARIS is a HPC cluster based on IBM's NeXtScale platform, incorporating the Intel[(R)] Xeon[(R)] E5 v2 processors (Ivy Bridge) and having a theoretical peak performance (R_{peak}) of 190.85 TFlops and a sustained performance (R_{max}) of 179.73 TFlops on the Linpack benchmark. With a total of 426 computing nodes, each incorporating two 10 core CPUs, it offers more than 8500 processor cores that are interconnected *via* an FDR Infiniband network. More details on GRNET's HPC service are available at https://hpc.grnet.gr.
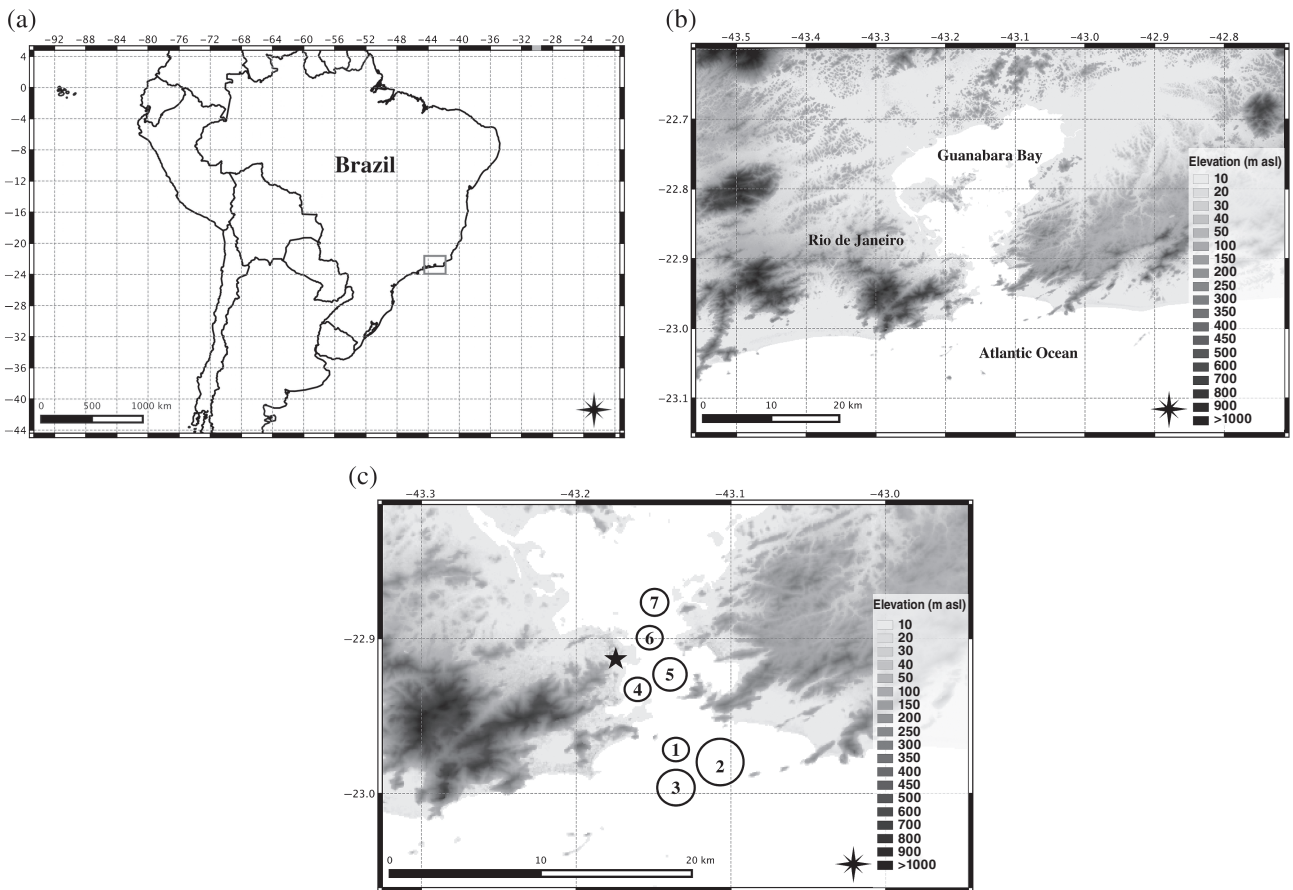
Figure 1. (a) Location map of the Guanabara Bay (rectangle) in southeast Brazil. Topographic maps of (b) the Guanabara Bay and (c) the Marina da Gloria (star) venue for the sailing events of the 2016 Olympic Games, with identification of the sailing courses (circles 1–7).

To address the needs of the present study, 946 172 core hours of ARIS were used. In particular, the operational implementation of AEOLUS-RIO2016 exploited the computing capacity of 300 processor cores, available on a daily basis. This allowed the model to be accelerated significantly, thus ensuring the timely delivery of the forecasts to the HOST, early in the morning (0630 BRT, UTC − 3).

3.1.1. Representation of the complex terrain

One of the key issues that had to be addressed during the development of the NWP system was the proper representation of the complex terrain of the target area (Figure 1(c)). In particular, for wind speed and direction forecasting, topography and land use have been reported to be of great importance (e.g. Kotroni and Lagouvardos, 2004; Pineda *et al.*, 2004; Lam *et al.*, 2006; Akylas *et al.*, 2007; Sertel *et al.*, 2009; Carvalho *et al.*, 2012; Santos-Alamillos *et al.*, 2013, 2015; De Meij and Vinuesa, 2014). Considering this, updated high resolution datasets for topography and land use were employed to substitute the standard ones of the WRF model.

For topography, the 90 m resolution Shuttle Topography Radar Mission (SRTM) data (Jarvis *et al.*, 2008) were used, replacing the default ~1 km US Geological Survey dataset. For land use, the European Space Agency's (ESA) GlobCover 2009 dataset (Arino *et al.*, 2010), with 300 m resolution, was employed. To allow for its ingestion in the WRF model, the land use categories of ESA GlobCover 2009 were remapped to the categories of the standard ~1 km resolution Moderate Resolution Imaging

Spectroradiometer (MODIS) International Geosphere Biosphere Programme (IGBP) dataset. The SRTM and ESA GlobCover datasets were only used in the innermost ultrahigh resolution (200 m) domain (Figure 1(c)), while the standard US Geological Survey and MODIS-IGBP datasets were used in the three outer domains (25, 5, 1).

3.2. Communication channels

Communication of the forecasts to the HOST was carried out using two channels, the key features of which were defined in collaboration with the athletes and their coaches in order to fulfil their particular needs.

3.2.1. Forecast briefings

Forecasts of half-hourly winds and two-hourly weather conditions were issued once daily, at approximately 0630 BRT, for each of the seven sailing courses (Figure 1(c)). An example of such a forecast, valid for 12 August 2016, is presented in Figure 2. As shown, a tabulated format was chosen for communicating information in a comprehensive, yet simple, way. This information included a detailed forecast of the wind conditions anticipated at each of the racing courses (Figure 2(a)) and an overview of the expected weather conditions (Figure 2(b)). Briefings were routinely issued for both the current day (24 h forecast) and the following day (48 h forecast).

Special post-processing routines were developed for the automatic production of the forecast briefings. The model grid points

(a)

Date: 12 August 2016
Event: Olympic Games, Rio 2016
Team: Hellenic Wind (Nacra GRE)

Meteo grnet

DETAILED WIND FORECAST: COPACABANA

Hour (BST)	Mean WD	WD Range	Mean WS	WS Range	WS Gust
09:30−10:00	W	253−264	13	11−13	13−18
10:00−10:30	WSW	246−256	13	12−13	13−14
10:30−11:00	WSW	244−254	12	12−13	13−14
11:00−11:30	SW	231−236	13	13−14	14−16
11:30−12:00	SW	228−233	15	14−15	14−16
12:00−12:30	SW	229−235	15	14−16	15−17
12:30−13:00	SW	229−239	16	15−17	16−18
13:00−13:30	SW	224−232	15	15−16	16−18
13:30−14:00	SW	226−231	15	14−16	15−17
14:00−14:30	SW	225−230	15	14−16	15−17
14:30−15:00	SW	222−227	15	14−16	17−18
15:00−15:30	SW	223−229	14	14−15	15−16
15:30−16:00	SW	221−228	13	13−14	14−15
16:00−16:30	SW	222−227	12	12−13	13−17
16:30−17:00	SW	218−225	12	12−13	13−16
17:00−17:30	SW	218−224	12	11−13	12−14
17:30−18:00	SW	218−223	12	11−13	12−14
18:00−18:30	SW	217−223	11	10−13	11−13
18:30−19:00	SW	216−223	11	10−13	11−14
19:00−19:30	SW	215−220	12	10−13	11−14
19:30−20:00	SW	217−220	11	10−12	12−13

(b)

Date: 12 August 2016
Event: Olympic Games, Rio 2016
Team: Hellenic Wind (Nacra GRE)

Meteo grnet

METEO INFO: COPACABANA

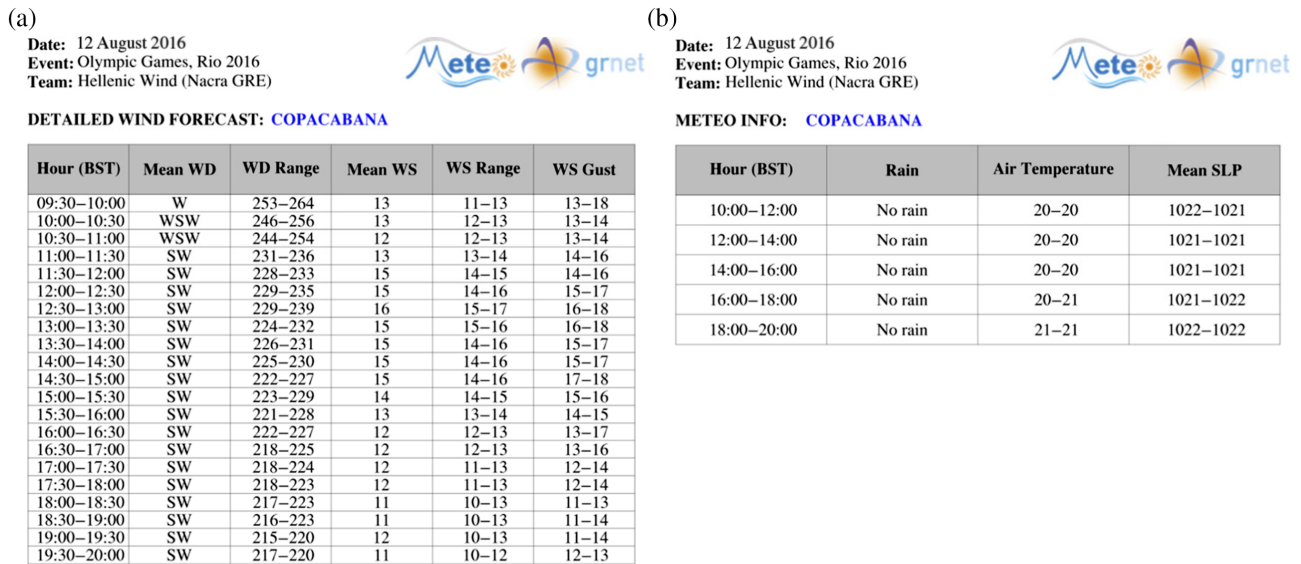| Hour (BST)	Rain	Air Temperature	Mean SLP
10:00−12:00	No rain	20−20	1022−1021
12:00−14:00	No rain	20−20	1021−1021
14:00−16:00	No rain	20−20	1021−1021
16:00−18:00	No rain	20−21	1021−1022
18:00−20:00	No rain	21−21	1022−1022

Figure 2. Forecast issued on the morning of 12 August 2016 for the Copacabana sailing course: (a) detailed forecast of the wind conditions; (b) an overview of the expected weather conditions. Forecasts were also routinely provided for the other six racing courses. [Colour figure can be viewed at wileyonlinelibrary.com].

falling within the boundaries of each racing course were first identified, and the wind parameters presented in Figure 2(a) were then derived over half-hourly intervals for the period from 0930 BRT to 2000 BRT. Following the needs of the HOST's athletes and coaches, these parameters included the dominant wind direction (Mean WD, descriptive), the wind direction range (WD Range, degrees north), the average wind speed (Mean WS, kn), the wind speed range (WS Range, kn) and the range of wind gusts (WS Gust, kn). As for the weather overview (Figure 2(b)), information was provided over two-hourly intervals and included rainfall (Rain) and variations in air temperature (Air Temperature) and mean sea-level pressure (Mean SLP). All the relevant tables were 'packed' into a single PDF file and were sent automatically to a mailing list containing the addresses of all the members of the HOST.

3.2.2. Web mapping application

A web-based application, encompassing advanced digital cartography technology, was employed for visualizing forecasts. A screenshot of the application, which was developed by GET Ltd using the open source software GET SDI Portal, is shown in Figure 3. The application was built using a centralized geographic information system (GIS) management platform in which all relevant data were routinely organized and stored in geospatial format (raster and/or vector). An open source spatial database and a GIS server were consequently used in order to provide the OGC compliant spatial services (Web Map Service, Web Feature Service) used by the web client for visualizing the geospatially formatted NWP system output, including wind, rainfall, mean sea-level pressure, air temperature and cloud cover. Advanced raster to vector SLD transformations were employed to allow for producing the vector wind arrows/barbs from the raster datasets. All datasets had time as an additional dimension in order to enable access to different forecast times. The easy-to-use interface of the web application provided several advanced spatial analysis functionalities, allowing the members of the HOST to zoom in and out, move back and forth in time, overlay different layers of information and obtain data at any point of the map by simply clicking on it.

4. Verification data and methodology

AEOLUS-RIO2016 forecasts were verified against wind measurements collected at four locations within the target area. These included the Santos Dumont International Airport (SBRJ: 22°54′37″ S, 43°9′46″ W) and three buoys (http://www.simcosta.furg.br) deployed within the Guanabara Bay (RJ1, 22°57′41.76″ S, 43°7′29.38″ W; RJ2, 22°55′55.13″ S, 43°8′52.37″ W; RJ3, 22°58′59.1″ S, 43°10′28.1″ W). Data were sampled at 60 and 30 min intervals for the SBRJ station and the buoys, respectively.

The verification of the NWP system was conducted in two stages. In the first stage, wind forecasts were verified over the period from 1 June to 30 June 2016. During this period, the WRF model was implemented experimentally with the default and the updated topography and land use datasets (Section 3.1.1). In the second stage, model performance was evaluated for the 11 day period of the Olympic sailing events, from 8 August to 18 August 2016, when AEOLUS-RIO2016 was operationally deployed. For each case, the verification procedure focused on the time period ranging from 0930 to 2000 BRT, for which forecasts were routinely provided to the HOST (Section 3.2.1).

The statistical measures used for the verification are (1) the bias error (B), (2) the root mean squared error (RMSE), (3) the wind bearing error (WBE) and (4) the magnitude of the vector error (MVE), computed using Equations (1)−(4) as reported in Spark and Connor (2004). Forecasted (F_i) and observed (O_i) wind data were paired using the nearest neighbour approach, in which the model grid point nearest to the measurement location was selected for extracting model data:

$$B = \frac{1}{N} \sum_{i=1}^{N} \left(F_i - O_i \right) \qquad (1)$$

$$\text{RMSE} = \sqrt{\frac{1}{N} \sum_{i=1}^{N} \left(F_i - O_i \right)^2} \qquad (2)$$

$$\text{WBE} = \frac{1}{N} \sum_{i=1}^{N} \left| F_i - O_i \right| \qquad (3)$$
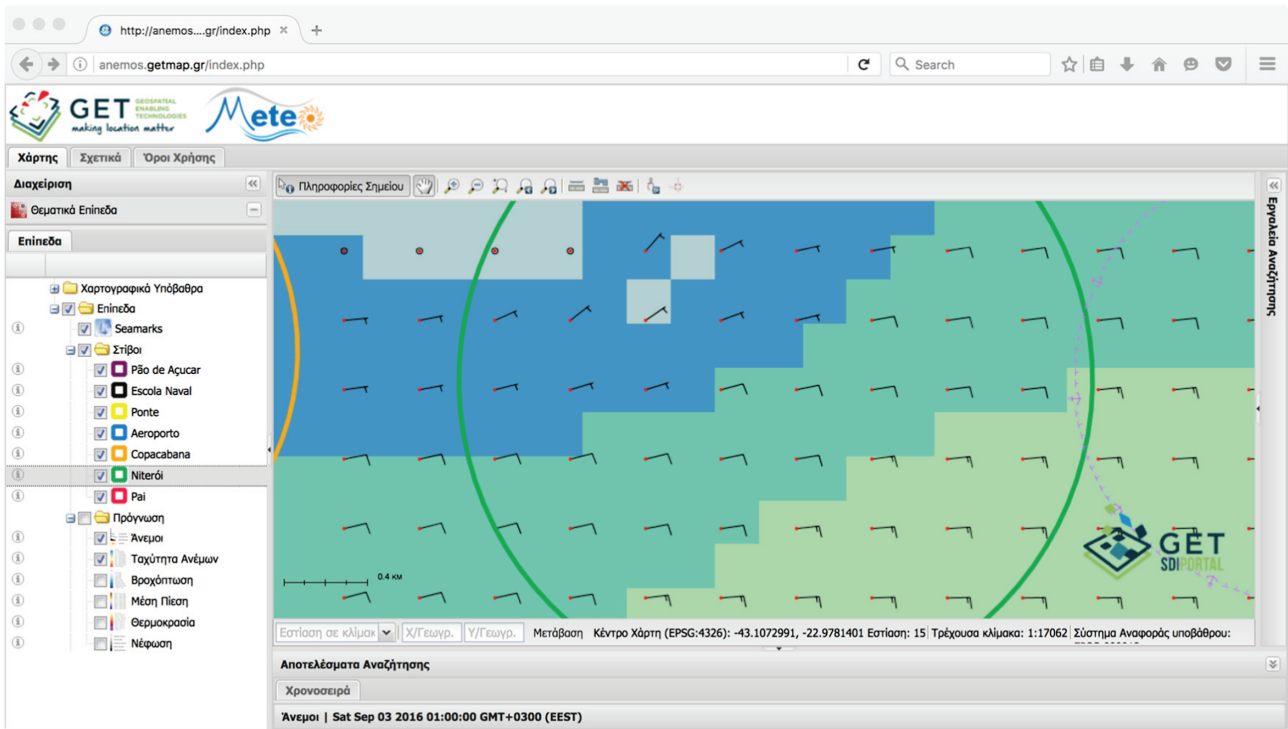
Figure 3. Screenshot of the web-based application used for the operational visualization of the forecasts. The interactive map is zoomed over the Niteroi racing course and shows wind barbs and wind speed. [Colour figure can be viewed at wileyonlinelibrary.com].

Table 1. Wind speed verification statistics for the experimental implementation period (1–30 June 2016), grouped by measurement location.

Location	B (m s^{-1})		RMSE (m s^{-1})		MVE (m s^{-1})	
	CNTL	TOPO	CNTL	TOPO	CNTL	TOPO
SBRJ	−0.2	**0.4**	1.3	**1.5**	0.9	**1.1**
RJ1	−1.0	**0.0**	2.2	**1.8**	1.6	**1.3**
RJ2	−0.5	**0.5**	1.6	**1.8**	1.1	**1.4**

Buoy RJ3 is not included due to data unavailability. Statistics are presented for the forecasts with the default (CNTL) and updated (TOPO) topography and land use datasets (see Section 3.1.1). Values appearing in bold indicate statistically significant differences (at $\alpha = 0.05$) between the scores of the competing datasets (i.e. CNTL and TOPO).

$$ \text{MVE} = \frac{1}{N} \sum_{i=1}^{N} \left| F_i - O_i \right| \qquad (4) $$

Regarding wind direction errors, these were computed using the approach described in Carvalho *et al.* (2012) to account for the fact that direction is a circular variable. In addition, the percentage of forecasts with a WBE not exceeding 20° was calculated, taking into account the particular importance of wind direction for sailing. Indeed, according to the *International Sailing Federation Race Management Manual* (ISAF, 2013), race officials should 'start thinking about a change of course when the wind shift turns out to be of 20° or more'.

5. Results

5.1. Experimental implementation period: 1–30 June 2016

Tables 1 and 2 summarize the verification of AEOLUS-RIO2016 wind forecasts during the experimental implementation period. In terms of the wind vector error (Table 1), it is evident that the use of the default topography and land use datasets (CNTL) resulted in underestimation, with biases ranging from −1.0 m s^{-1}

for RJ1 to −0.2 m s^{-1} for SBRJ. This underestimation was waived when the SRTM and GlobCover datasets were used (TOPO). In particular for the RJ1 site, where the largest CNTL errors were computed, the updated topography and land use datasets allowed the RMSE and the MVE values to be reduced. Overall, the TOPO forecast errors for wind speed were found to be consistent among the three measurement sites, not exceeding 2 m s^{-1} for RMSE and 1.5 m s^{-1} for the MVE.

The employment of the SRTM and GlobCover datasets for representing topography and land use, respectively, had a more profound positive influence on wind direction forecasts, compared to wind speed. As shown in Table 2, the replacement of the default datasets allowed the RMSE to be reduced, in particular for the two buoys that showed the largest errors in the CNTL forecasts. More importantly, TOPO forecasts were found to provide better directional guidance than CNTL forecasts, as highlighted by the increase in the percentage of wind bearing forecasts within 20° of measurements.

5.2. Olympic sailing events period: 8–18 August 2016

The performance of AEOLUS-RIO2016 during the sailing events of the Olympic Games is summarized in Table 3. For

Table 2. As Table 1 but for wind direction verification statistics.

Location	B (°)		RMSE (°)		WBE (°)		% WBE < 20°	
	CNTL	TOPO	CNTL	TOPO	CNTL	TOPO	CNTL	TOPO
SBRJ	−3.8	**0.7**	40.5	**39.3**	25.3	**24.6**	63	63
RJ1	−16.5	**−18.6**	59.2	**49.0**	46.1	**36.0**	25	35
RJ2	−21.4	**−16.7**	52.5	**49.7**	38.7	**34.2**	35	43

Values appearing in bold indicate statistically significant differences (at $\alpha = 0.05$) between the scores of the competing datasets (i.e. CNTL and TOPO).

Table 3. Wind speed and direction verification measures for each measurement site, for each day (0930–2000 BRT) of the sailing events' period (8–18 August 2016).

Day	SBRJ		RJ1		RJ2		RJ3	
	MVE (m s^{-1})	WBE (°)	MVE (m s^{-1})	WBE (°)	MVE (m s^{-1})	WBE (°)	MVE (m s^{-1})	WBE (°)
8	1.6	25.5	0.8	19.3	1.3	30.3	1.2	29.0
9	1.7	14.3	1.4	105.7	1.3	63.5	1.7	89.4
10	1.2	43.9	2.3	23.7	4.5	39.0	1.4	30.3
11	1.0	26.6	1.8	18.7	2.1	24.0	3.1	30.9
12	2.8	68.8	2.3	52.4	3.2	66.2	1.5	37.4
13	2.5	29.1	1.5	41.1	2.1	50.3	1.9	32.7
14	0.8	22.1	1.3	40.7	0.6	36.0	1.3	39.2
15	1.1	139.1	3.3	66.7	2.4	123.4	3.6	67.5
16	0.7	7.5	1.1	46.0	0.8	36.4	0.9	53.1
17	2.2	77.6	0.8	44.0	1.5	52.8	1.7	100.7
18	0.8	16.6	1.8	27.5	1.0	25.8	2.8	18.9

clarity, only the metrics of MVE and WBE, for each day of the sailing events' period, are presented. Concerning wind speed, forecast errors were found to range from 0.7 m s^{-1} (SBRJ, 16 August) to 4.5 m s^{-1} (RJ2, 10 August). Lower MVE values were computed for the SBRJ and RJ1 sites, lying to the northern part of the Guanabara Bay, than for the RJ2 and RJ3 sites, located at the mouth of the bay. The computed biases (not shown) indicate that wind speeds were overestimated. Overall, for the entire period of the sailing events, AEOLUS-RIO2016 provided wind speed forecasts with an average MVE ranging from 1.5 m s^{-1} for SBRJ to 2.0 m s^{-1} for RJ3. These values are of similar magnitude to similar previous studies (Spark and Connor, 2004; Pezzoli and Bellasio, 2014).

Focusing on wind direction, the computed WBE values indicate a rather significant variation in model performance both throughout the sailing events' period and between the considered sites (Table 3). In general, AEOLUS-RIO2016 provided better direction guidance for the SBRJ and RJ1 sites than for RJ2 and RJ3. This is highlighted in the reported WBE values, as well as in the percentage of forecasts showing a WBE lower than 20° (not shown). Indeed, it was found that for SBRJ and RJ1, this percentage equalled 53% and 30%, respectively, whereas for RJ2 and RJ3 the calculated values were found to be equal to 24% and 10%, respectively. On a daily basis, wind direction errors exhibited absolute values ranging (1) from 7.5° to 139.1° for SBRJ, (2) from 18.7° to 105.7° for RJ1, (3) from 24.0° to 123.4° for RJ2 and (4) from 18.9° to 100.7° for RJ3. The WBE values averaged over the entire period were approximately 37°, 44° and 47° for SBRJ, RJ1, and RJ2 and RJ3, respectively.

5.2.1. Impact of initial conditions

Closer examination of Table 3 reveals that there were specific days for which AEOLUS-RIO2016 did not succeed in providing useful wind direction guidance. In particular, the largest

WBE values were computed for 9 August, 12 August, 15 August and 17 August. Considering this, an additional set of forecasts was carried out, with the aim of identifying the causes for this model performance, which contrasts results obtained during the experimental implementation period (Section 5.1). In this context, AEOLUS-RIO2016 was reimplemented for the above days, using the 0000 UTC 0.5° × 0.5° spatial resolution and 6 h temporal resolution data of the European Centre for Medium-Range Weather Forecasts (ECMWF). Apart from the initialization data, all other model settings were kept the same, so that any difference between the GFS and the ECMWF initialized forecasts should be attributed to initial conditions.

Tables 4 and 5 summarize the results obtained from the above described sensitivity exercise. Clearly, the use of ECMWF instead of GFS data for initializing AEOLUS-RIO2016 does induce improvements in wind forecasts. This is mostly highlighted in the case of wind direction, for which the ECMWF-driven model showed significantly better verification scores compared to the GFS-driven forecasts. As shown in Table 5, RMSE values were reduced by about 9–15% and the WBE values by approximately 5–15% when the ECMWF data were employed. Most importantly, however, the ECMWF-driven AEOLUS-RIO2016 was found to provide improved wind direction guidance, as highlighted by the increase in the percentage of forecasts exhibiting WBE values lower than or equal to 20°.

6. Conclusions

Environmental conditions and weather are of great importance for the design of sports performance. Sailing, in particular, is a characteristic example of a sport where athletes rely heavily on detailed and reliable wind information for elaborating their strategy, both before and during a competitive event. Acknowledging this, the National Observatory of Athens, in collaboration with

Table 4. Wind speed verification statistics averaged over selected days (9, 12, 15 and 17 August 2016) of the sailing events' period, grouped by measurement location.

Location	B (m s^{-1})		RMSE (m s^{-1})		MVE (m s^{-1})	
	GFS	ECMWF	GFS	ECMWF	GFS	ECMWF
SBRJ	1.6	**1.2**	2.5	**2.1**	2.1	**1.7**
RJ1	0.3	**−0.5**	2.7	**3.5**	1.9	**2.3**
RJ2	0.7	**0.6**	2.7	**2.8**	2.1	**1.9**
RJ3	−0.5	**−0.8**	2.9	**2.9**	2.0	**2.0**

Statistics are presented for the forecasts initialized with GFS and ECMWF data. Values appearing in bold indicate statistically significant differences (at $\alpha = 0.05$) between the scores of the competing datasets (i.e. GFS and ECMWF).

Table 5. As Table 4 but for wind direction verification statistics.

Location	B (°)		RMSE (°)		WBE (°)		% WBE < 20°	
	GFS	ECMWF	GFS	ECMWF	GFS	ECMWF	GFS	ECMWF
SBRJ	−6.4	25.5	91.8	90.9	65.8	62.3	43	54
RJ1	−25.8	**−8.4**	82.3	**70.5**	66.4	**56.2**	16	21
RJ2	−3.3	**−9.0**	94.9	**84.9**	74.0	**62.9**	21	28
RJ3	−7.2	**−8.0**	83.1	**74.8**	72.8	**60.9**	2	20

Values appearing in bold indicate statistically significant differences (at $\alpha = 0.05$) between the scores of the competing datasets (i.e. GFS and ECMWF).

Geospatial Enabling Technologies Ltd and Greek Research and Technology Network SA, voluntarily developed an ultrahigh resolution wind forecasting system, AEOLUS-RIO2016, for supporting the efforts of the Hellenic Olympic Sailing Team (HOST) during the 2016 Summer Olympic Games, held in Rio de Janeiro, Brazil.

Two different fully automated channels, designed to meet the requirements of athletes and coaches, were set up for communicating wind forecasts. These included concise briefings and an advanced web-based mapping application. Briefings, summarizing the expected wind and weather conditions at each racing area, were routinely constructed and forwarded *via* email to all the members of the HOST. Athletes and coaches were also granted exclusive access to a user-friendly mapping application, which allowed for the visualization of the forecasts using advanced web-based cartographic techniques.

AEOLUS-RIO2016 was first experimentally implemented in June 2016. This trial implementation period focused on verifying model performance and evaluating the impact of using alternative and up-to-date terrestrial data. The analysis conducted revealed that the employment of the state-of-the-art Shuttle Topography Radar Mission (SRTM) topography and the European Space Agency (ESA) GlobCover land use datasets did improve model performance in terms of wind forecasting. In particular and more importantly, it was found that AEOLUS-RIO2016 was able to provide improved wind direction guidance, summarized in the percentage of forecasts that exhibited a wind bearing error lower than or equal to 20°, when the default model datasets for topography and land use were replaced by the corresponding SRTM and ESA GlobCover. This finding is of particular importance, highlighting the necessity to employ high resolution and up-to-date terrestrial datasets that ensure the proper representation of the area of interest, especially when ultrahigh resolution grids are adopted.

Considering the operational deployment of AEOLUS-RIO2016 during the sailing events' period of the games, comparisons against observations showed an overall satisfactory performance. However, there were specific days during which the model failed characteristically to forecast wind conditions in the Guanabara Bay. Further analysis showed that one of the potential causes for this lay in the initialization of the model. More specifically, when European Centre for Medium-Range Weather Forecasts data where used instead of Global Forecast System data for initializing AEOLUS-RIO2016, a substantial improvement in the provided wind forecasts was obtained. This was particularly evident for wind direction, for which the employment of alternative initialization data resulted in significant improvements in wind direction guidance. Nevertheless, it should be highlighted that the low performance of the model on specific days could also imply weaknesses in terms of the representation of particular synoptic- and local-scale meteorological setups. Considering this, it is intended to extend the present work by analysing model performance for different meteorological conditions.

Summarizing, this study highlights the added value that numerical weather prediction (NWP) models can provide in the context of sports' performance design, and especially in competitive sailing. Taking into consideration the rapid development of high performance computing infrastructures, the adoption of horizontal grid resolutions as high as a few hundred metres will be a feasible option in the upcoming years. Based on our findings, special attention should be paid to the proper representation of the targeted area, in terms of topography and/or land use distribution, as well as to the initialization of the model. The reported statistically significant improvements in model performance provide strong evidence that the common issue of wind overestimation in Weather Research and Forecasting simulations (e.g. Zhang *et al*., 2013; Hariprasad *et al*., 2014) could be tackled by adopting a high horizontal grid spacing and by carefully selecting large-scale forcing data. Besides these, extensive evaluation of NWP models should be continuously carried out, allowing for the identification of weaknesses and ways for overcoming these.

Acknowledgements

wind forecasting system. The authors are also grateful to NCEP (USA) for providing initial and forecast field data, which allowed the operational implementation of AEOLUS-RIO2016 at the National Observatory of Athens. The research leading to these results has been co-funded by the European Commission under the H2020 Research Infrastructures contract no. 675121 (project VI-SEEM).

References

Akylas E, Kotroni V, Lagouvardos K. 2007. Sensitivity of high resolution operational weather forecasts to the choice of the planetary boundary layer scheme. *Atmos. Res.* **84**: 49–57.

Arino O, Ramos J, Kalogirou V, Defourny P, Achart F. 2010. GlobCover 2009. *Proceedings of the ESA-iLEAPS-EGU Earth Observation for Land−Atmosphere Interaction Science*, 3–5 November 2010, European Space Agency: Frascati.

Bethwaite F. 2011. *High Performance Sailing, Faster Racing Techniques*. Adlard Coles Nautical: London.

Cairns JA. 1984. The effect of weather on football attendances. *Weather* **39**: 87–90.

Carvalho D, Rocha A, Gomez-Gesteira M, Santos C. 2012. A sensitivity study of the WRF model in wind simulation for an area of high wind energy. *Environ. Modell. Softw.* **33**: 23–34.

De Carvalho DG, Neto JAB. 2016. Microplastic pollution of the beaches of Guanabara Bay, Southeast Brazil. *Ocean Coastal Manage.* **128**: 10–17.

De Meij A, Vinuesa JF. 2014. Impact of SRTM and Corine land cover data on meteorological parameters using WRF. *Atmos. Res.* **143**: 351–370.

Diafas V, Kaloupsis S, Bachev V, Dimakopoulou E, Diamanti V. 2006. Weather conditions during Athens Olympic rowing and flat-water canoe-kayak regatta at the Olympic rowing center Schinias. *Kinesiology* **38**: 72–77.

Dudhia J. 1989. Numerical study of convection observed during the Winter Monsoon Experiment using a mesoscale two-dimensional model. *J. Atmos. Sci.* **46**: 3077–3107.

Ely FR, Cheuvron SN, Roberts WO, Montain SJ. 2007. Impact of weather conditions on Marathon-running performance. *Med. Sci. Sports Exercise* **39**: 487–493.

Fujita TT. 1986. Mesoscale classifications: their history and their application to forecasting. In *Mesometeorology and Forecasting*, Ray PS (ed). American Meteorological Society: Boston, MA; 18–35.

Giannaros TM, Melas D, Ziomas I. 2017. Performance evaluation of the Weather Research and Forecasting (WRF) model for assessing wind resource in Greece. *Renewable Energy* **102A**: 190–198.

Hariprasad KB-RR, Srinivas CV, Bagavath Singh A, Vijaya Bhaskara Rao S, Baskaran R, Venkatraman B. 2014. Numerical simulation and intercomparison of boundary layer structure with different PBL schemes in WRF using experimental observations at a tropical site. *Atmos. Res.* **145**: 27–44.

Houghton D, Campbell F. 2008. *Wind Strategy*, 3rd edn. Wiley Nautical: Chichester, UK.

INMET. 2015. Weather information for the Olympic and Paralympic Games in Rio de Janeiro. Report, National Institute for Meteorology (INMET): Brazil; 44 https://inside.fei.org/system/files/RIO%20 Weather%20forecast_0.pdf (accessed 20 July 2016).

ISAF. 2013. *ISAF Race Management Manual*. International Sailing Federation (ISAF): Southampton, UK; 213.

Janjic ZI. 1994. The step-mountain Eta coordinate model: further developments of the convection, viscous sublayer, and turbulence closure schemes. *Mon. Weather Rev.* **122**: 927–945.

Jarvis A, Reuter HI, Nelson A, Guevara E. 2008. Hole-filed SRTM for the globe Version 4, available from the CGIAR-CSI SRTM 90 m database. http://srtm.csi.cgiar.org (accessed 20 July 2016).

Kain JS. 2004. The Kain−Fritsch convective parameterization: an update. *J. Appl. Meteorol.* **43**: 170–181.

Kioutsioukis I, De Meij A, Jakobs H, Katragkou E, Vinuesa J-F, Kazandzidis A. 2016. High resolution WRF ensemble forecasting for irrigation: multivariate evaluation. *Atmos. Res.* **167**: 156–174.

Koletsis I, Giannaros TM, Lagouvardos K, Kotroni V. 2016. Observational and numerical study of the Vardaris wind regime in northern Greece. *Atmos. Res.* **171**: 107–120.

Kotroni V, Lagouvardos K. 2004. Evaluation of MM5 high-resolution real-time forecasts over the urban area of Athens, Greece. *J. Appl. Meteorol.* **43**: 1666–1678.

Lam JSL, Lau AKH, Fung JCH. 2006. Application of refined land-use categories for high resolution mesoscale atmospheric modeling. *Boundary Layer Meteorol.* **119**: 236–288.

Ma Y, Gao R, Xue Y, Yang Y, Wang X, Liu B, *et al.* 2013. Weather support for the 2008 Olympic and Paralympic sailing events. *Adv. Meteorol.* **2013**: 289284.

Matzarakis A, Fröhlich D. 2015. Sport events and climate for visitors – the case of FIFA World Cup in Qatar 2022. *Int. J. Biometeorol.* **59**: 481–486.

Mlawer EJ, Taubman SJ, Brown PD, Iacono MJ, Clough SA. 1997. Radiative transfer for inhomogeneous atmospheres: RRTM, a validated correlated-*k* model for the longwave. *J. Geophys. Res.* **102**: 16663–16682.

Morris BJ, Phillips ID. 2009. The effect of weather conditions on the Oxford−Cambridge University Boat Race. *Meteorol. Appl.* **16**: 157–168.

Pezzoli A, Bellasio R. 2014. Analysis of wind data for sports performance design: a case study for sailing sports. *Sports* **2**: 99–130.

Pezzoli A, Cristofori E, Gozzini B, Marchisio M, Padoan J. 2012. Analysis of the thermal comfort in cycling athletes. *Procedia Eng.* **34**: 433–438.

Pezzoli A, Moncalero M, Boscolo A, Cristofori E, Giacometto F, Gastaldi S, *et al.* 2010. The meteo-hydrological analysis and the sport performance: which are the connections? The case of the XXI Winter Olympic Games, Vancouver 2010. *J. Sports Med. Phys. Fitness* **50**: 19–20.

Pineda N, Jorga O, Jorge J, Baldasano JM. 2004. Using NOAA AVHRR and SPOT VGT data to estimate surface parameters: application to a mesoscale meteorological model. *Int. J. Remote Sens.* **25**: 129–143.

Rothfusz LP, McLaughlin MR, Rinard SK. 1998. An overview of NWS weather support for the XXVI Olympiad. *Bull. Am. Meteorol. Soc.* **79**: 845–860.

Santos-Alamillos FJ, Pozo-Vasquez D, Ruiz-Arias JA, Lara-Fanego V, Tovar-Pescador J. 2013. Analysis of WRF model wind estimate sensitivity to parameterization choice and terrain representation in Andalusia (Southern Spain). *J. Appl. Meteorol. Climatol.* **52**: 1592–1609.

Santos-Alamillos FJ, Pozo-Vasquez D, Ruiz-Arias JA, Tovar-Pescador J. 2015. Influence of land-use misrepresentation on the accuracy of WRF wind estimates: evaluation of GLCC and CORINE land-use maps in southern Spain. *Atmos. Res.* **157**: 17–28.

Schroter RC, Marlin DJ. 1995. An index of the environmental thermal load imposed on exercising horses and riders by hot conditions. *Equine Vet. J.* **27**: 16–22.

Sertel A, Robock A, Ormeci C. 2009. Impacts of land cover data quality on regional climate simulations. *Int. J. Climatol.* **30**: 1942–1953.

Skamarock WC, Klemp JB, Dudhia J, Gill DO, Barker DM, Duda MG *et al.* 2008. A description of the Advanced Research WRF version 3. Technical Note TN-475+STR, NCAR: Boulder, CO; 125.

Soares-Gomes A, Da Gama BAP, Baptista Neto JA, Freire DG, Cordeiro RC, Machado W, *et al.* 2016. An environmental overview of Guanabara Bay, Rio de Janeiro. *Reg. Stud. Mar. Sci.* **8**(2): 319–330. https://doi.org/10.1016/j.rsma.2016.01.009.

Spark E, Connor GJ. 2004. Wind forecasting for the sailing events at the Sydney 2000 Olympic and Paralympic Games. *Weather Forecasting* **19**: 181–199.

Spellman G. 1996. Marathon running – an all-weather sport? *Weather* **51**: 118–125.

Tewari M, Chen F, Wang W, Dudhia J, LeMone MA, Mitchell K *et al.* 2004. Implementation and verification of the Unified NOAH land surface model in the WRF model. *Proceedings of the 20th Conference on Weather Analysis and Forecasting/16th Conference on Numerical Weather Prediction*, Seattle, WA, 10-15 January 2004. American Meteorological Society: Seattle, WA.

Thompson G, Field PR, Rasmussen RM, Hall WD. 2008. Explicit forecasts of winter precipitation using an improved bulk microphysics scheme. Part II: Implementation of a new snow parameterization. *Mon. Weather Rev.* **136**: 5095–5115.

Thorne JE. 1977. The effect of weather on sport. *Weather* **32**: 258–268.

Zeri M, Oliveira-Junior JF, Lyra GB. 2011. Spatiotemporal analysis of particulate matter, sulphur dioxide and carbon monoxide concentrations over the city of Rio de Janeiro, Brazil. *Meteorol. Atmos. Phys.* **113**: 139–152.

Zhang H, Pu Z, Zhang X. 2013. Examination of errors in near-surface temperature and wind from WRF numerical simulations in regions of complex terrain. *Weather Forecasting* **28**: 893–914.